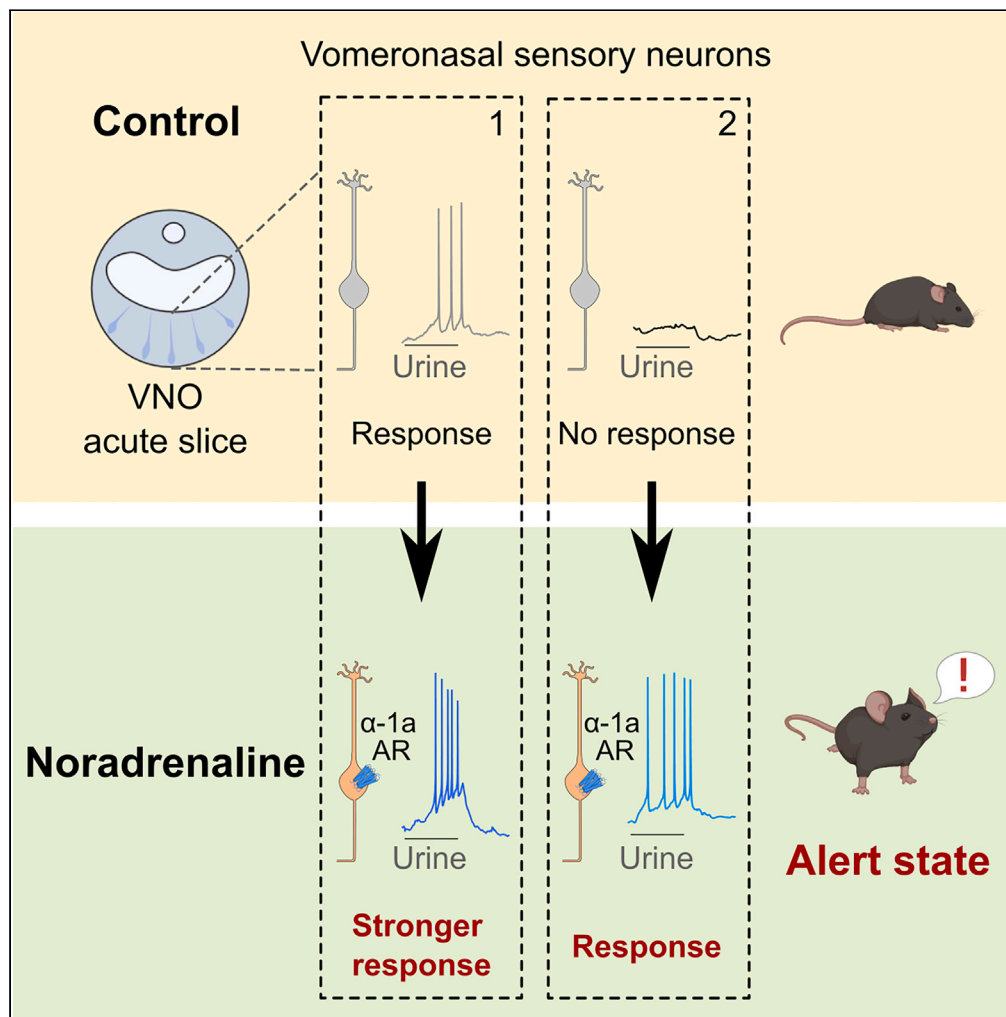**Article**

Noradrenaline modulates sensory information in mouse vomeronasal sensory neurons

Cesar Adolfo Sánchez Triviño, Andres Hernandez-Clavijo, Kevin Y. Gonzalez-Velandia, Simone Pifferi, Anna Menini

s.pifferi@staff.univpm.it (S.P.)
anna.menini@sissa.it (A.M.)

Highlights

Noradrenaline increases the excitability of vomeronasal sensory neurons

The action of noradrenaline is mediated by the activation of alpha 1 receptors

Catecholaminergic fibers innervate the sensory epithelium of the VNO

Article

Noradrenaline modulates sensory information in mouse vomeronasal sensory neurons

Cesar Adolfo Sánchez Triviño,[1,5] Andres Hernandez- Clavijo,[1,2,5] Kevin Y. Gonzalez-Velandia,[1,4] Simone Pifferi,[3,*] and Anna Menini[1,6,*]

SUMMARY

During the induction of the body's alert state, the sympathetic system modulates sensory modalities and fine-tunes peripheral organs for improved stimulus detection. We explored noradrenaline (NA)'s role in modulating signaling in vomeronasal sensory neurons (VSNs), responsible for detecting pheromones and other semiochemicals. In current-clamp recordings, NA increased the firing frequency in response to natural stimuli of responsive VSNs and induced spiking activity in previously unresponsive neurons. Current injections into VSNs showed an increase in firing frequency during NA application. Combining transcriptomic analysis, electrophysiology, Ca^{2+} imaging, and a pharmacological approach, we identified alpha 1 adrenergic receptors as crucial for NA-induced firing frequency increases in VSNs. Immunohistochemistry revealed catecholaminergic fibers in the vomeronasal sensory epithelium, suggesting localized NA release near VSNs. This study unveils NA as a key regulator of VSN signaling, shedding light on the intricate interplay between the sympathetic nervous system and chemosensory processing, advancing our understanding of sensory modulation.

INTRODUCTION

Sensory systems are modulated by various substances even at the level of peripheral sensory organs.[1] Modulatory substances include neurotransmitters, hormones, and neuropeptides that may influence the activity of receptor cells in various sensory systems, including olfactory sensory neurons (OSNs) of the olfactory epithelium in many vertebrate species.[2,3]

The autonomic nervous system is one of the most relevant regulatory systems in the body, managing the internal environment and engaging the organism in either a "flight-or-fight" response or in a "rest-and-digest" state, depending on which division of the autonomic system is more active. The sympathetic system is mainly responsible for inducing an alert state in the body through the release of the neurotransmitter noradrenaline (NA) and the hormone adrenaline, both activating adrenergic receptors.[4,5] During the induction of the body's alert state, the sympathetic system also influences several sensory modalities and fine-tunes peripheral organs for improved stimulus reception. For example, in the visual system, NA triggers pupil dilation, controlling the amount of light entering the eye to stimulate the retina.[6] In the peripheral auditory system, the sympathetic system controls cochlear blood flow and NA has been shown to protect outer hair cells against noise-induced damage.[7,8] In taste receptor cells, NA enhances calcium-activated chloride currents, inhibits outward potassium currents, and increases intracellular calcium concentration contributing to modifications of cells' excitability.[9,10] In the peripheral olfactory system, adrenaline enhances odorant contrast by regulating the sensitivity of OSNs.[11–13] However, little is known about the potential regulation of the peripheral vomeronasal system, primarily responsible for detecting pheromones and other semiochemicals, by the sympathetic system. Some studies showed that the vomeronasal organ (VNO) is functionally innervated by the sympathetic system.[14–16]

The VNO is one of the chemosensory organs used by many mammals to detect chemical stimuli in the environment, a crucial ability that plays a significant role in survival, communication, and interaction with the external world.[17] The VNO is composed of two main regions: a non-sensory region containing non-sensory epithelium and blood vessels, and a sensory region, the vomeronasal sensory epithelium. These structures run parallel along the anteroposterior axes, with the lumen space between them filled with mucus and in direct contact with the nasal cavity.[17–19]

The VNO non-sensory region is largely composed of venous blood vessels and smooth muscle fibers.[15,20] Its principal function is to provide the mechanical force necessary for the chemicals dissolved in the mucus to enter into the VNO lumen, a process known as VNO pumping.

[1]Neurobiology Group, SISSA, Scuola Internazionale Superiore di Studi Avanzati, 34136 Trieste, Italy
[2]Department of Chemosensation, Institute for Biology II, RWTH Aachen University, 52074 Aachen, Germany
[3]Department of Experimental and Clinical Medicine, Università Politecnica delle Marche, 60126 Ancona, Italy
[4]Present address: Department of Neuroscience, University of Rochester School of Medicine and Dentistry, Rochester, NY 14642, USA
[5]These authors contributed equally
[6]Lead contact
*Correspondence: s.pifferi@staff.univpm.it (S.P.), anna.menini@sissa.it (A.M.)
https://doi.org/10.1016/j.isci.2024.110872

Recent evidence has enhanced our understanding of the pumping mechanism in the VNO, demonstrating the crucial involvement of the sympathetic system.[15] This system innervates the intricate smooth muscle fibers and vasculature, inducing repetitive contractions that drive the pumping action, introducing chemicals into the VNO.[15,21] The pumping mechanism involves the alternating activation of NA-sensitive muscle fibers and acetylcholine-activated muscle fibers, which, due to their different orientations within the organ, generate opposing effects on the volume of the lumen.[15]

In the sensory epithelium, vomeronasal sensory neurons (VSNs) detect chemicals that enter the VNO lumen and bind to specific vomeronasal receptor proteins at the apical microvilli of the VSNs. Each VSN expresses only one or few members of three families of G protein coupled vomeronasal receptors: vomeronasal type 1 receptor (V1Rs), vomeronasal type 2 receptors (V2Rs), or formylated peptide receptors (FPRs) and each receptor binds different ligands. The binding activates a phospholipase C (PLC)-based signaling cascade, leading to membrane depolarization and subsequent firing of action potentials. This firing activity is sent to the accessory olfactory bulb (AOB) in the brain for further processing, modulating the physiological and behavioral responses of the animal.[20,22–28]

Here, to investigate the potential role of NA in modulating signaling in VSNs, we recorded the firing activity of VSNs in acute slices of the mouse VNO. Surprisingly, we found that not only NA cause an increase in firing frequency in VSNs responsive to a natural stimulus composed of diluted mouse urine, but also elicits a response in VSNs that did not initially respond to urine, indicating a modulatory effect of NA on VSNs responsiveness. Moreover, we found that, independently of the transduction mechanism, NA affects the generation of action potential in VSNs, as current injection experiments showed an increase in firing frequency during NA application, in the absence of urine stimuli. Through transcriptomic analysis of previously published data from the whole VNO single cell RNA-seq data,[29] we identified the expression in VSNs of Adra1a, encoding the alpha 1a adrenergic receptor. We obtained a functional validation of the involvement of alpha 1 adrenergic receptors in the modulatory effect of NA through electrophysiological and calcium imaging experiments, combined with a pharmacological approach. Our experimental findings establish alpha 1, likely alpha 1a, as the primary adrenergic receptor type activated by NA in VSNs. Furthermore, by immunohistochemistry, we provide evidence that the sensory epithelium of the VNO is innervated by catecholaminergic fibers indicating that NA could be released in close proximity to VSNs.

RESULTS

Noradrenaline increases the firing frequency of responses to natural stimuli in vomeronasal sensory neurons

To evaluate the NA's potential impact on VSNs during their response to natural stimuli, we performed current-clamp whole-cell recordings from VSNs in acute murine VNO slices, using diluted mouse urine (1:50) as a natural stimulus. Indeed, urine is often used as a stimulus for VSNs because it is a rich source of pheromones and ligands that interact with vomeronasal receptors and activate the transduction cascade leading to action potential generation.[24,27,30–33] We measured spiking activity induced by diluted urine application in 42% of the viable VSNs (10 out of 24). Subsequently, we applied 50 μM NA and, after 3 min, challenged the same recorded VSNs, whether initially responsive or not, with a second diluted urine application identical to the first one. We measured that 70% (7 out of 10) of the initially responsive VSNs exhibited an increased mean spiking frequency when stimulated a second time in the presence of NA and returned to the initial value after 5 min wash-out (Figures 1A and 1E). Control experiments showed that repetitive urine stimulation in the same time frame (3 and 5 min after the first stimulation) and in the absence of NA had a stable spiking activity (Figure 1C). Normalization of the firing frequency in the presence of NA to the value in control for each tested VSN (n = 10) showed an overall increase in the firing frequency induced by NA (Figure 1D). In NA-responding VSNs (n = 7), the average spiking frequency in response to urine rose from 1.37 ± 0.83 Hz under control conditions to 2.48 ± 1.30 Hz during NA application, returning to 1.31 ± 0.78 Hz after washout (n = 7; Figures 1A and 1E). Surprisingly, 36% (5 out of 14) initially unresponsive VSNs showed a clear spiking activity in response to urine when NA was present (Figures 1B and 1F). Importantly, the effect of NA on spiking activity following urine stimulation was entirely reversible upon washout (Figure 1). These results clearly show that NA can increase VSNs' responsiveness to their natural ligands.

Noradrenaline increases the firing frequency by activating alpha-1 adrenergic receptors

Changes in firing activity driven by NA during responses to natural stimuli in VSNs could arise from two mechanisms: i) modulation of elements within the complex and heterogeneous signal transduction cascade, and/or ii) modulation of the action potential machinery. To assess if NA's effect on VSNs could be observed independently of signal transduction activation, we bypassed the transduction cascade by using direct current injections to activate the action potential machinery in VSNs.

In the first set of experiments, we applied repetitive 3 pA current steps lasting 3 s, at 1 min intervals (to prevent adaptation, as previously described by Sarno et al.,[32] under three conditions: control, NA application, and subsequent washout (Figures 2A and 2B). Remarkably, NA application led to a progressive increase in action potential frequency, which became statistically significant 3 min after applying NA and subsequently decreased during washout (Figures 2A and 2B). Based on these results, subsequent experiments were conducted by applying current steps in control conditions, at least 3 min after NA application, and at least 5 min after the beginning of the washout (Figure 2C; see STAR Methods). In another set of experiments, we expanded the range of current stimulation step amplitudes from 0 to 6 pA (Figure 2D), increasing by 1 pA increments. NA significantly increased the frequency of action potentials elicited by current injections ranging from 3 to 6 pA (Figure 2D). Specifically, using 3 pA current steps, the average firing frequency increased from 2.0 ± 1.1 Hz in the control state to 2.8 ± 1.4 Hz in the presence of NA (n = 10), subsequently returning to 1.8 ± 1.0 Hz after washout (n = 10; Figure 2D). To further analyze the NA effect, we normalized the firing frequency in the presence of NA to the value in control for each VSN and further confirmed the increase in firing frequency induced by NA in the range of current steps from 3 to 6 pA (Figure 2E). NA had no significant impact on the resting membrane
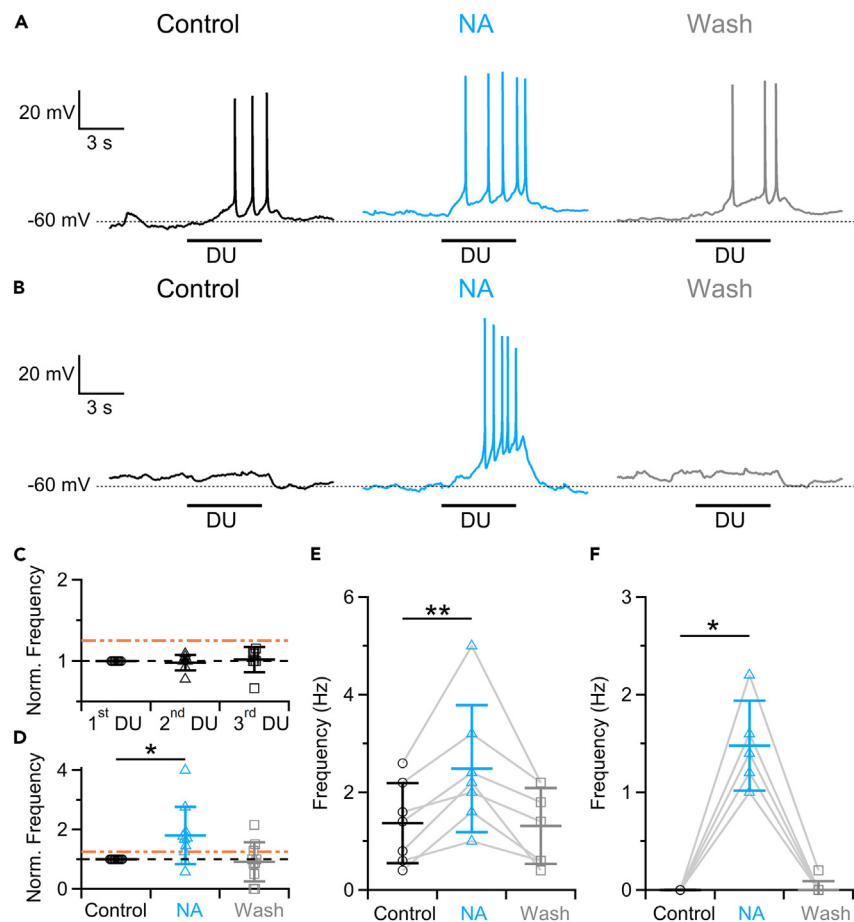
Figure 1. Noradrenaline increases urine-induced action potential firing in VSNs

(A and B) Representative whole-cell current-clamp recordings from VSNs stimulated for 5 s with diluted urine (DU, 1:50) in control condition, during the application of 50 µM NA and after washout. Recordings with NA started 3 min after the application of NA and washout was measured 5 min after removal of NA. Neuron in (B) responded to urine only during the application of NA. Bars at the bottom indicate the time of urine application.

(C) Control experiments in urine-responsive VSNs in the absence of NA. Scatterplot with the averages ±SD of the ratio between firing frequencies measured in response to urine applications at 3 and 5 min after the first stimulation and the frequency measured during the first stimulation. $n = 9$ VSNs; $p = 0.28$ for 2nd DU and $p = 0.07$ for 3rd DU, One sample sign test. The orange dashed line indicates 1.25.

(D) Scatterplot with the averages ±SD of normalized firing frequencies during the application of NA and after wash out from experiments as in (A). Also, neurons unresponsive to NA are included. The dashed line, at 1.25, indicates the threshold set to select a VSN with increased firing frequency with respect to control. $n = 10$ VSNs; $p = 0.027$ for NA and $p = 0.69$ for wash, One sample t-test.

(E and F) Scatterplots with averages ±SD of the firing frequencies from experiments as in (A) and (B) respectively. (E) $n = 7$ VSNs responsive to NA; $p = 0.00917$ (Control-NA), $p = 1$ (control-wash) t-test with Bonferroni's correction after ANOVA for repeated measurements $p = 0.0007$. (F) $n = 5$ VSNs initially unresponsive to urine; $p = 0.026$ (Control-NA), $p = 1$ (control-wash) Demsar test after Friedman test $p = 0.0087$.

potential measured at zero-current injection (RMP), indicating that NA does not modulate the resting ionic conductances (-72 ± 4 mV in control, -69 ± 5 mV in the presence of NA, -69 ± 5 mV after washout ($n = 10$; Figure 2F). Although some VSNs exhibited a large depolarization during NA application, there was no correlation between the change in firing frequency induced by NA at 3 pA current injection and the change of RMP ($r^2 = 0.38$, $p = 0.076$, $n = 10$).

Overall, 67% of VSNs (18 out of 27) tested with 3 pA current injection displayed reversible increases in firing frequency during NA application.

These results collectively demonstrate that NA exerts a direct effect on action potential generation in VSNs, producing a firing frequency increase.

To assess which adrenergic receptors mediate the effect of NA, we examined the transcriptional profile of adrenergic receptors in mature VSNs (Figures 3A and 3B) analyzing previously published scRNA-seq data from the VNO.[29] After filtering (see STAR Methods) 14,851 single cells were kept in the dataset to be analyzed. Such cells were separated into 11 clusters and were annotated following the same nomenclature and marker genes used by Katreddi et al.[29] A cluster containing 2,327 cells and expressing *Omp* transcript was annotated as mature VSNs
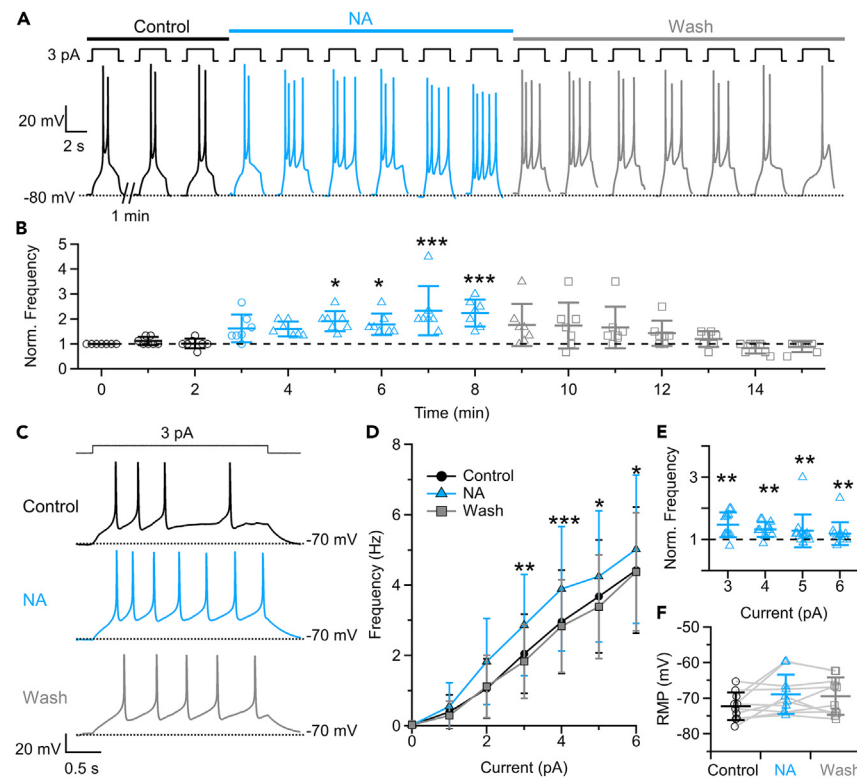
Figure 2. Noradrenaline increases spike frequency in response to current injections in VSNs

(A) Representative whole-cell current-clamp recordings from a VSN repetitively stimulated with 3 pA current steps for 3 s at 1 min intervals in control, during the application of 50 μM NA, and during washout. Steps at the top indicate the time of current injections.

(B) Scatterplot with the averages ±SD of normalized firing frequencies of each stimulation with respect to the first stimulation as a function of time from experiments as in (A). n = 7 VSNs; p = 0.01, p = 0.02, p = 0.0005, p = 0.0006, p = 0.0006 for 3, 4, 5, and 6 min after NA application, Demsar test after Friedman test p = 1.73*10-6.

(C) Representative current-clamp recordings from VSNs stimulated with 3 pA current steps for 3 s in control, during the application of 50 μM NA and after washout. Recordings with NA started 3 min after the application of NA and washout was measured 5 min after removal of NA.

(D) Averages ±SD of firing frequencies as a function of current injection amplitude in the indicated conditions. n = 10 VSNs; for 1 pA, p = 0.426 (C-NA), p = 1 (C-wash); for 2 pA, p = 0.082 (C-NA), p = 1 (C-wash); for 3 pA, p = 0.004 (C-NA), p = 0.51 (C-wash); for 4 pA, p < 0.001 (C-NA), p = 1 (C-wash); for 5 pA, p = 0.012 (C-NA), p = 0.127 (C-wash); for 6 pA, p = 0.032 (C-NA), p = 1 (C-wash), paired t test with Bonferroni correction after mixed model two-way ANOVA p < 0.001.

(E) Scatterplot with the averages ±SD of normalized firing frequencies (spike frequency in the presence of NA/control spike frequency) as a function of current injected between 3 and 6 pA from experiments in (D). n = 10 VSNs; p = 0.006 for 3 pA, p = 0.006 for 4 pA, p = 0.003 for 5pA, p = 0.003 for 6 pA, One sample sign test.

(F) Scatterplot with the averages ±SD of the resting membrane potentials (RMP) in the indicated conditions. n = 10 VSNs, p = 0.06 Friedman test.

(mVSN). We found that *Adra1a*, the transcript for alpha 1a adrenergic receptors, was the most abundant among adrenergic receptor transcripts in mVSNs (Figure 3B), indicating that alpha 1a is likely to be the main receptor type activated by NA in VSNs.

To investigate the involvement of alpha 1 receptors in the response to NA, we measured the effects of selective alpha 1 receptor agonists and antagonists on VSN excitability (Figure 4). Methoxamine (50 μM), a selective agonist of alpha 1 receptors,[35–37] increased the firing frequency, indicating that the activation of alpha 1 receptors produces an enhancement of VSNs excitability (Figures 4A–4C), without modifying the resting membrane potential (Figure 4D). In addition, there was no correlation between the change in firing frequency induced by methoxamine at 3 pA current injection and the change of RMP ($r^2 = 0.47$, $p = 0.13$, $n = 6$). By using prazosin (2.5 μM), a selective antagonist of alpha 1 receptors,[4,38,39] application of 50 μM NA failed to increase firing frequency elicited by current injections and did not affect the resting membrane potential (n = 5–6; Figures 4E–4H).

In summary, these findings show that NA modulates VSN firing frequency by acting on alpha-1 adrenergic receptors.

Noradrenaline induces intracellular Ca²⁺ increase

It is well established that the binding of agonists to alpha-1 adrenergic receptors leads to an increase in cytosolic Ca^{2+}. This occurs through the activation of G_q proteins that stimulate PLC that, in turn, hydrolyzes phosphatidylinositol 4,5-bisphosphate (PIP_2) into inositol 1,4,5-trisphosphate (IP_3) and diacylglycerol (DAG). The binding of IP_3 to receptors on the endoplasmic reticulum triggers Ca^{2+} release into the
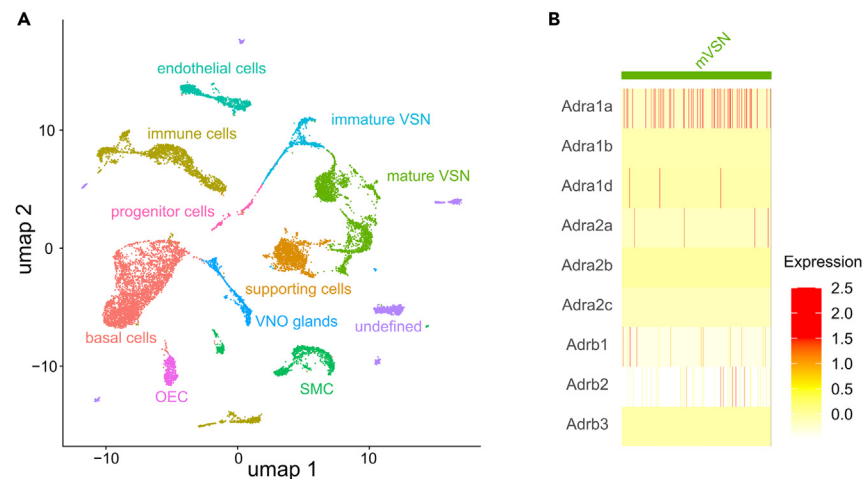
Figure 3. Expression of adrenergic receptors in VSNs

(A) Visualization of the clustering results from the whole VNO scRNA-seq data produced in Katreddi et al.[29] on a Uniform Manifold Approximation and Projection (UMAP) plot. The cell type annotation of each cluster is noted on the color key legend and labels. SMC: smooth muscle cell, OEC: olfactory ensheathing cell.

(B) Heatmap showing expression levels[34] of the transcripts of adrenergic receptors in mature VSNs.

cytoplasm.[4,38,40] To investigate whether the stimulation of VSNs with NA produces a rise in intracellular Ca^{2+}, which could potentially contribute to the molecular mechanisms that produce a higher firing frequency, we conducted Ca^{2+} imaging experiments on dissociated mouse VSNs loaded with the Ca^{2+} indicator Fluo4-AM.

To distinguish viable VSNs from other cells and exclude non-viable neurons, we used a depolarizing high K^+ solution and selectively analyzed only VSNs responding to high K^+ with a Ca^{2+} increase. Application of 50 μM NA for 20 s did not significantly increase fluorescence while with 100 μM NA stimulation a notable increase in fluorescence was observed in several viable dissociated VSNs. This rise in fluorescence persisted across three consecutive NA stimulations at an interstimulus interval of 3 min (n = 18; Figures 5A and 5B). Overall, 52% of VSNs (48 out of 93) exhibited an increase in intracellular Ca^{2+} concentration in response to NA stimulation. To evaluate if the rise in fluorescence was mediated by alpha 1 receptors, we applied the antagonist prazosin (2.5 μM), which effectively blocked the Ca^{2+} increase induced by NA in dissociated VSNs (Figures 5C and 5D). Furthermore, we explored whether the alpha 1 agonist methoxamine (50 μM) could induce intracellular Ca^{2+} increases in dissociated VSNs similar to NA. Our findings revealed that dissociated VSNs responded to methoxamine with an elevation in intracellular Ca^{2+} concentration (Figures 5E and 5F).

These results collectively demonstrate that NA induces Ca^{2+} increases in VSNs through the activation of alpha-1 receptors.

We reasoned that, if the increase in firing frequency induced by NA in current-clamp whole-cell recordings is indeed caused by an intracellular Ca^{2+} increase, then reducing the Ca^{2+} increase by dialyzing the cytosol of VSNs with an intracellular solution containing the rapid Ca^{2+} chelator BAPTA, should decrease, or abolish, the effect of NA on VSNs. Thus, we recorded from VSNs in VNO acute slices and measured the effect of NA on firing frequencies induced by current steps by using BAPTA instead of EGTA as a Ca^{2+} chelator inside the patch pipette. We found that, when the rapid Ca^{2+} chelator BAPTA was used in the patch pipette, NA failed to significantly increase the firing frequency elicited by current injections (Figures 5G–5I).

Taken together, these results suggest that a Ca^{2+} increase induced after the activation of alpha 1 receptors by NA may be involved in the increase of firing frequency in VSNs, although additional experiments are required to establish whether this is the general mechanism of NA effect.

Sympathetic nerve fibers in the vomeronasal sensory epithelium

To investigate if NA could be released in the direct proximity of VSNs, we investigated if the sensory epithelium in the VNO is innervated by catecholaminergic fibers. Indeed, previous studies showed a functional innervation of the VNO by the sympathetic system in mice and hamsters[14,16] and a recent work found that the release of NA by sympathetic fibers controls the contraction of smooth muscles in the non-sensory epithelium responsible for VNO pumping playing a pivotal role in the stimulus intake.[15] We labeled coronal and horizontal cryosections of adult VNOs with antibodies targeting tyrosine hydroxylase (TH). In both sectioning planes, coronal or horizontal, a comprehensive morphology of the VNO can be observed, including: the non-sensory epithelium characterized by a large blood vessel; the sensory epithelium, and the lumen, a mucus-filled cavity separating the two epithelia (Figure 6). Consistent with the findings of Hamacher et al.,[15] a dense network of TH positive nerve fibers was observed in the non-sensory epithelium of the VNO (Figures 6B, 6C and 6C$_a$). Importantly, we identified TH positive nerve fibers also innervating the basal region of the vomeronasal sensory epithelium (Figures 6B, 6C and 6C$_b$; arrows). The presence of catecholaminergic innervation within the sensory epithelium implies a potential for a localized and precise release of NA in close proximity to VSNs. These results show that catecholaminergic fibers of the sympathetic system innervate both the sensory and non-sensory epithelia of the mouse VNO.
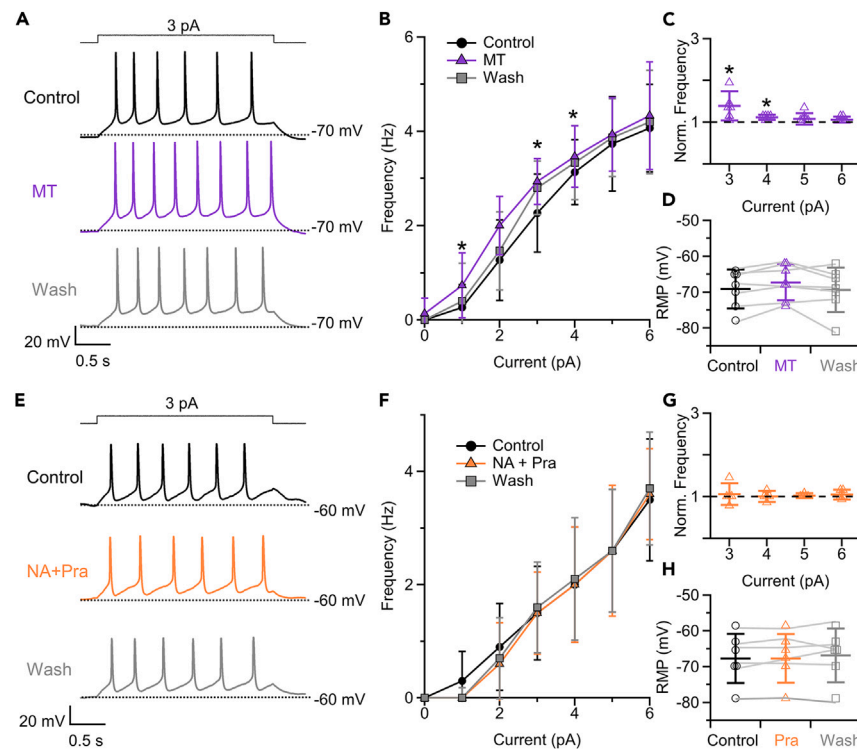
Figure 4. Noradrenaline increases the spike frequency of VSNs through alpha-1 adrenergic receptors

(A) Representative current-clamp recordings from a VSN stimulated with 3 pA current steps for 3 s in control, during the application of 50 μM methoxamine (MT) and after washout. Recordings with methoxamine started 3 min after its application and washout was measured 5 min after removal.

(B) Average ±SD of firing frequency as a function of current injection in the indicated conditions ($n = 7$ VSNs; for 1 pA, $p = 0.038$ (C-MT), $p = 1$ (C-wash); for 2 pA, $p = 0.059$ (C-MT), $p = 0.887$ (C-wash); for 3 pA, $p = 0.032$ (C-MT), $p = 0.247$ (C-wash); for 4 pA, $p = 0.012$ (C-MT), $p = 0.227$ (C-wash); for 5 pA, $p = 0.609$ (C-MT), $p = 0.1$ (C-wash); for 6 pA, $p = 0.306$ (C-MT), $p = 1$ (C-wash), paired t test with Bonferroni correction after mixed model two-way ANOVA $p = 0.002$).

(C) Scatterplot with the averages ±SD of normalized firing frequencies (spike frequency in the presence of MT/control spike frequency) as a function of current injected between 3 and 6 pA from experiments in (B). $n = 7$ VSNs; $p = 0.03$ for 3 pA, $p = 0.03$ for 4 pA, One sample sign test.

(D) Scatterplot with the average ±SD of the resting membrane potential (RMP) in the indicated conditions. $n = 7$ VSNs; $p = 0.094$ ANOVA for repeated measurements.

(E) Representative current-clamp recordings from a VSN stimulated with 3 pA current steps for 3 s in control, after the application of 50 μM NA and 2.5 μM prazosin (Pra) and after washout. NA and prazosin were applied for 3 min and washout was measured 5 min after removal.

(F) Average ±SD of firing frequency as a function of current injection in the indicated conditions. $n = 5$ VSNs; $p = 0.4$ mixed model two-way ANOVA.

(G) Scatterplot with the averages ±SD of normalized firing frequencies (spike frequency in the presence of NA + Pra/control spike frequency) as a function of current injected between 3 and 6 pA from experiments in (E). $n = 5$ VSNs; $p > 0.05$ One sample sign test.

(H) Scatterplot with the average ±SD of the resting membrane potentials (RMP) in the indicated conditions. $n = 6$ VSNs; $p = 0.56$ ANOVA for repeated measurements.

DISCUSSION

In this study, we demonstrate that NA increases VSN action potential firing through the activation of alpha 1 adrenergic receptors, leading to an increase in intracellular Ca^{2+} concentration. Furthermore, through the analysis of available single-cell transcriptomic data, we show that mature VSNs predominantly express alpha 1a adrenergic receptors. In addition, we show that catecholaminergic fibers innervate the sensory epithelium, indicating that NA could be released near VSNs.

In current-clamp whole-cell recordings, we measured spiking activity in response to natural stimuli in mouse diluted urine, which contains a rich blend of pheromones, in 42% of the viable VSNs. This percentage is in agreement with electrophysiological experiments from several laboratories that have demonstrated that approximately 30–50% of VSNs respond to urine blends[24,25,41–44]

NA caused an increase in the firing frequency in 70% of the neurons responding to urine and the frequency returned to the initial value after the washout of NA, showing that the increase was reversible. Surprisingly, also 36% of the initially unresponsive neurons fired action potentials in response to urine when NA was present and returned to be unresponsive after NA washout, providing an additional clear demonstration that NA modulates responses to natural stimuli by increasing the responsiveness of VSNs. A similar threshold shift induced by other compounds has also been described in OSNs. For example, in amphibians, cannabinoids have been shown to lower the firing threshold of OSNs, thus enhancing their responsiveness.[45,46] Moreover, neuropeptide Y and gonadotropin-releasing hormone modulate the sensitivity
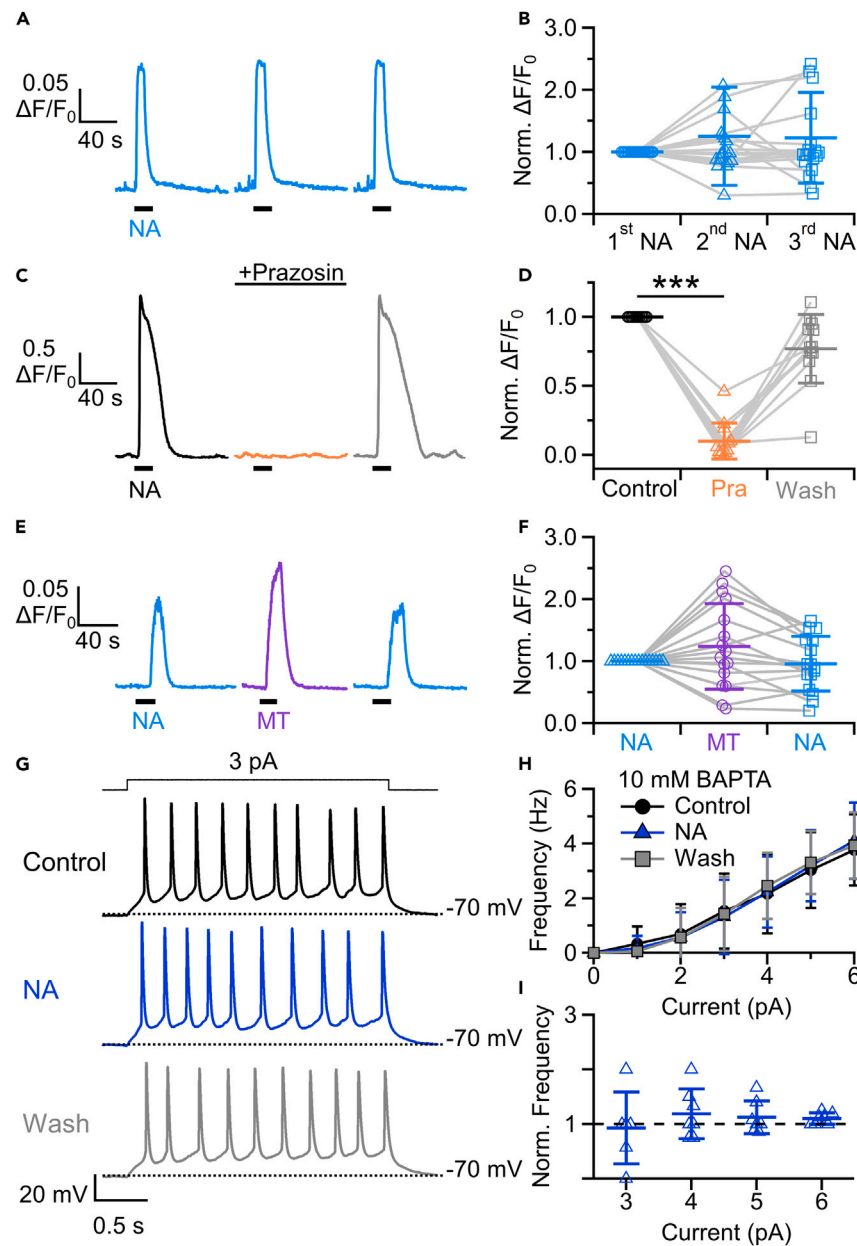
Figure 5. Alpha 1 adrenergic receptor activation increases intracellular calcium in VSNs

(A, C, and E) Representative recordings of cytosolic Ca^{2+} signals from VSNs in response to: (A) three repetitive stimulations with 100 μM NA (20 s); (C) stimulations with 100 μM NA (20 s) in control, during the application of 2.5 μM prazosin and after its washout; (E) Stimulations with 100 μM NA (20 s) or 50 μM methoxamine (MT, 20 s). The interval between stimulations was 3 min.

(B, D, and F) Scatterplot with average ±SD of normalized changes in fluorescence intensity following stimulations as indicated in (A, C, E) respectively. All data were normalized to the peak value obtained from the first stimulation. (B) n = 18 VSNs; p = 0.805 Friedman test. (D) n = 12 VSNs; p = 5.3×10^{-6} (Con-Pra), p = 0.082 (Con-wash) Demsar test after Friedman test p = 1.5×10^{-5}. (F) n = 16 VSNs; p = 0.144 Friedman test.

(G) Representative whole-cell current-clamp recordings from a VSN in a VNO coronal slice repetitively stimulated with 3 pA current steps for 3 s at 1 min intervals in control, during the application of 50 μM NA and after washout. The intracellular solution contained the rapid Ca^{2+} chelator BAPTA (10 mM). Recordings with NA started 3 min after its application and washout was measured 5 min after removal.

(H) Average ±SD of firing frequencies as a function of current injection in the indicated conditions (n = 7 VSNs; p = 0.994 mixed model two-way ANOVA).

(I) Scatterplot with the averages ±SD of normalized firing frequencies (spike frequency in the presence of NA/control spike frequency) as a function of current injected between 3 and 6 pA from experiments in (H). n = 7 VSNs; p > 0.05 One sample sign test.
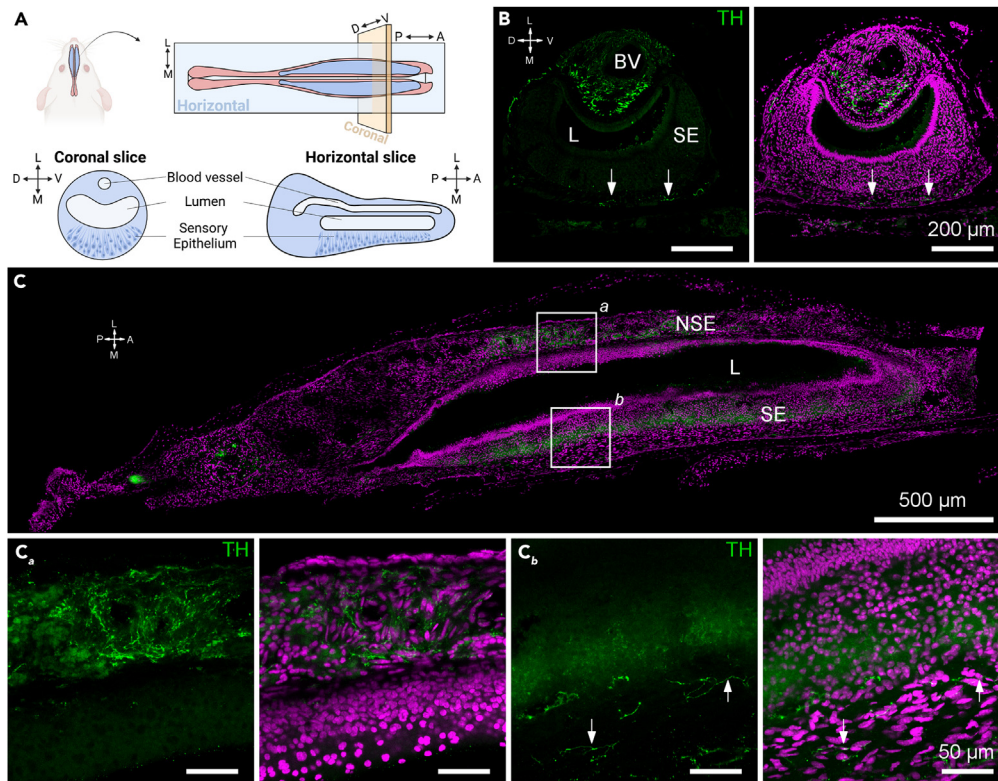
Figure 6. Catecholaminergic fibers innervate the VNO sensory epithelium

(A) Schematic representation of the VNO and the tissue distribution after coronal or horizontal sectioning.

(B and C) Immunostaining against tyrosine hydroxylase (TH) enzyme (green) on coronal (B) and horizontal (C) sections of the VNO. White squares in *C* denote the zoomed in areas for the non-sensory epithelium (C_a) and sensory epithelium (C_b). White arrows indicate the presence of TH-positive fibers in the basal zone of the sensory epithelium. Note the high innervation by TH-positive fibers on the non-sensory epithelium. Nuclei were stained with DAPI (magenta). BV: blood vessel; SE: sensory epithelium; NSE: non-sensory epithelium; L: lumen.

of OSNs in amphibians.[47,48] These findings, along with our data, demonstrate that the regulation of peripheral chemosensory neurons by internally released substances occurs in various systems.

As the binding of ligands to vomeronasal receptors first activates transduction cascades that may lead to action potential firing, NA modulation of the responses may occur at various stages during the transduction cascade and/or on ion channels producing action potentials. To bypass the transduction cascade and therefore the activation of specific vomeronasal receptors, we performed current-clamp experiments by using current steps. In these experimental conditions, NA caused a reversible increase in firing frequency in 67% of neurons (tested with 3 pA current steps). Although we cannot exclude the possibility that NA produces effects on components of the transduction cascade, these results demonstrate that NA affects the generation of action potentials causing an increase in firing frequency. The modulation of the transduction cascade could be relevant to increasing the receptor potential above the threshold in VSNs that respond to natural stimuli only after NA application. In this scenario, the NA intracellular signaling could induce post-translational modifications of receptors, G proteins, or ion channels such as TRPC2, TMEM16A, or TMEM16B increasing their sensitivity.

We investigated the expression of adrenergic receptors in VSNs with several approaches: by analyzing publicly available VNO single-cell RNA-seq data[29] and by performing electrophysiological and Ca^{2+}-imaging experiments combined with pharmacological compounds. Single-cell transcriptomic data revealed that mature VSNs predominantly express Adra1a, encoding the alpha 1a adrenergic receptor. From a functional point of view, although we could not validate the involvement of alpha 1a, because selective agonists or antagonists are unknown, we used selective compounds for alpha 1 receptors: the agonist methoxamine and the antagonist prazosin.[39] Methoxamine mimicked the increase in firing frequency in current-clamp experiments measured with NA stimulation and prazosin blocked such increase, confirming the activation by NA of alpha 1 receptors in VSNs. Since it is well known that alpha 1 receptor activation leads to an increase in cytosolic Ca^{2+}[4,38,40] we provided a further demonstration of the activation of alpha 1 receptors in VSNs by NA by performing Ca^{2+} imaging experiments on dissociated cells from the VNO. Indeed, stimulation with NA caused a clear increase in intracellular Ca^{2+} concentration in 52% of the tested VSNs that was mimicked by the selective alpha 1 agonist methoxamine and blocked by the selective antagonist prazosin.

Is the NA-induced increase in intracellular Ca^{2+} involved in the higher VSN excitability? In current-clamp experiments, when we reduced the increase in intracellular Ca^{2+} using the fast Ca^{2+} chelator BAPTA in the intracellular solution, we did not measure any increase in firing

frequency induced by NA, indicating that a Ca^{2+} increase may be involved in the higher VSN excitability. However, additional experiments are needed to fully understand the role of intracellular Ca^{2+} in NA-mediating signaling. In particular, it will be important to clarify if the intracellular Ca^{2+} rise is due to entry from the extracellular side and/or from release from internal stores.

It is of interest to note that in the peripheral olfactory system, adrenaline plays a role in enhancing odorant contrast by regulating the sensitivity of OSNs. Indeed,[13] demonstrated that adrenaline modulates action potential firing and induces a negative shift in the activation curve of voltage-gated Na^+ channels in sensory neurons of the main olfactory epithelium. Their study showed the involvement of beta-adrenergic receptors in the soma of OSNs. Upon binding to their agonists, these receptors trigger the synthesis of cAMP, leading to the subsequent activation of protein kinase A, which in turn could modulate voltage-gated Na^+ channels in OSNs. Interestingly, catecholamines enhance stimulus responses in both OSNs and VSNs by using distinct pathways: beta-adrenergic receptors in OSNs and alpha1 adrenergic receptors in VSNs.

Where is NA released within the vomeronasal sensory epithelium? While it is conceivable that there may be a systemic release of NA during states of arousal in the animal, there is also evidence indicating that the sympathetic system innervates the mouse and hamster VNOs.[14–16] A recent study by Hamacher et al.[15] reported the abundant presence of catecholaminergic fibers in the non-sensory epithelium of the mouse VNO and demonstrated that adrenergic stimulation controls the pumping activity of the VNO, contributing to the regulation of pheromone concentration reaching the organ. Here, we showed that catecholaminergic fibers not only innervate the non-sensory epithelium but also the basal region of the sensory epithelium of the VNO. This sympathetic innervation within the sensory epithelium suggests the possibility of a localized release of NA in close proximity to VSNs. Moreover, the shared innervation of both sensory and non-sensory epithelia, suggests the potential for synchronized release of NA within the VNO, thereby coordinating the uptake of stimuli with higher excitability of VSNs thus improving the detection of pheromones or other semiochemicals. However, it is important to note that the basal region of the sensory epithelium is composed of basal cells, smooth muscle cells (SMCs), blood vessels, and axon bundles from VSNs, among other cell types, and any of these could be the direct target of catecholaminergic fibers in the sensory epithelium. A detailed synaptic labeling of catecholaminergic fibers in the VNO would provide a better understanding of the main targets of NA in the sensory epithelium.

The overall action of NA in the control of vomeronasal signaling also depends on its modulation of the AOB, where signals from VSNs undergo further processing.[3,27] NA is released within the AOB from fibers originating in the locus coeruleus.[49] Several studies have demonstrated that NA induces concentration-dependent changes between the excitation and inhibition of mitral and granule cells through the activation of alpha 1 and alpha 2 adrenergic receptors ultimately resulting in a dual effect of NA on mitral cells' activity.[50–56] Furthermore, Doyle and Meeks[53] revealed the modulation of mitral cell activity is not uniform but is selective for the stimuli present during NA release, suggesting that different mitral cells respond distinctively to NA stimulation. However, a better understanding of NA's role in the modulation of AOB requires the physiological stimulation of noradrenergic fibers that could be obtained for example by using optogenetic tools.

In summary, our data provide evidence that NA can be released near VSNs and increase the spiking frequency of VSNs through the activation of alpha 1a adrenergic receptors, leading to a cytosolic increase in Ca^{2+} levels. This study shows that NA is a crucial regulator of VSN signaling and provides a foundation for future work investigating molecular aspects underlying NA modulation and interactions between the sympathetic nervous system and chemosensory processing.

Limitations of the study

In our study, several questions remain unanswered. Determining whether NA selectively influences specific subsets of VSNs (e.g., V1R, V2R, or FPR-expressing VSNs), and/or the detection of particular classes of signal molecules (e.g., high or low molecular weight molecules) would yield valuable insights, also related to heterogeneous responses in AOB mitral cells, Doyle and Meeks.[53] Furthermore, confirming whether the same nerve fibers innervate both sensory and non-sensory epithelia would support the hypothesis of coordinated stimulus uptake and VSN sensitivity regulation driven by NA. Investigating the precise temporal and spatial dynamics of NA on VSNs, would require the use of genetic tools for stimulating neurotransmitter release in the intact tissue, thus avoiding artifacts associated with an external perfusion system stimulation.

RESOURCE AVAILABILITY

Lead contact

Further information and requests for resources should be directed to and will be fulfilled by the lead contact, Anna Menini (anna.menini@sissa.it).

Materials availability

This study did not generate new unique reagents or mouse lines.

Data and code availability

- All data reported in this article will be shared by the lead contact upon request.
- This article does not report the original code.
- Any additional information required to reanalyze the data reported in this article is available from the lead contact upon request.

AUTHOR CONTRIBUTIONS

DECLARATION OF INTERESTS

STAR★METHODS

Detailed methods are provided in the online version of this paper and include the following:

- KEY RESOURCES TABLE
- EXPERIMENTAL MODEL AND STUDY PARTICIPANT DETAILS
  - Animals and ethical approval
- METHOD DETAILS
  - Electrophysiological recordings from VSNs in acute VNO slices
  - Calcium imaging from dissociated VSNs
  - Single-cell RNA sequencing data analysis
  - Immunohistochemistry
  - Chemicals
- QUANTIFICATION AND STATISTICAL ANALYSIS

REFERENCES

1. McGann, J.P. (2015). Associative learning and sensory neuroplasticity: how does it happen and what is it good for? Learn. Mem. *22*, 567–576. https://doi.org/10.1101/lm.039636.115.

2. Bryche, B., Baly, C., and Meunier, N. (2021). Modulation of olfactory signal detection in the olfactory epithelium: focus on the internal and external environment, and the emerging role of the immune system. Cell Tissue Res. *384*, 589–605. https://doi.org/10.1007/s00441-021-03467-y.

3. Manzini, I., Schild, D., and Di Natale, C. (2022). Principles of odor coding in vertebrates and artificial chemosensory systems. Physiol. Rev. *102*, 61–154. https://doi.org/10.1152/physrev.00036.2020.

4. Graham, R.M. (1990). Adrenergic receptors: structure and function. Cleve. Clin. J. Med. *57*, 481–491. https://doi.org/10.3949/ccjm.57.5.481.

5. McCorry, L.K. (2007). Physiology of the Autonomic Nervous System. Am. J. Pharmaceut. Educ. *71*, 78.

6. Ostrin, L.A., and Glasser, A. (2010). Autonomic drugs and the accommodative system in rhesus monkeys. Exp. Eye Res. *90*, 104–112. https://doi.org/10.1016/j.exer.2009.09.015.

7. Tian, C., Yang, Y., Wang, R., Li, Y., Sun, F., Chen, J., and Zha, D. (2024). Norepinephrine protects against cochlear outer hair cell damage and noise-induced hearing loss via α2A-adrenergic receptor. BMC Neurosci. *25*, 5. https://doi.org/10.1186/s12868-024-00845-4.

8. Tian, C., and Zha, D. (2022). Sympathetic Nervous System Regulation of Auditory Function. Audiol. Neurootol. *27*, 93–103. https://doi.org/10.1159/000517452.

9. Herness, M.S., and Sun, X.D. (1999). Characterization of chloride currents and their noradrenergic modulation in rat taste receptor cells. J. Neurophysiol. *82*, 260–271. https://doi.org/10.1152/jn.1999.82.1.260.

10. Herness, S., Zhao, F.L., Kaya, N., Lu, S.G., Shen, T., and Sun, X.D. (2002). Adrenergic signalling between rat taste receptor cells. J. Physiol. *543*, 601–614. https://doi.org/10.1113/jphysiol.2002.020438.

11. Firestein, S., and Menini, A. (1999). The smell of adrenaline. Nat. Neurosci. *2*, 106–108. https://doi.org/10.1038/5661.

12. Hall, R.A. (2011). Autonomic modulation of olfactory signaling. Sci. Signal. *4*, pe1. https://doi.org/10.1126/scisignal.2001672.

13. Kawai, F., Kurahashi, T., and Kaneko, A. (1999). Adrenaline enhances odorant contrast by modulating signal encoding in olfactory receptor cells. Nat. Neurosci. *2*, 133–138. https://doi.org/10.1038/5686.

14. Ben-Shaul, Y., Katz, L.C., Mooney, R., and Dulac, C. (2010). In vivo vomeronasal stimulation reveals sensory encoding of conspecific and allospecific cues by the mouse accessory olfactory bulb. Proc. Natl. Acad. Sci. USA *107*, 5172–5177. https://doi.org/10.1073/pnas.0915147107.

15. Hamacher, C., Degen, R., Franke, M., Switacz, V.K., Fleck, D., Katreddi, R.R., Hernandez-Clavijo, A., Strauch, M., Horio, N., Hachgenei, E., et al. (2024). A revised conceptual framework for mouse vomeronasal pumping and stimulus sampling. Curr. Biol. *34*, 1206–1221.e6. https://doi.org/10.1016/j.cub.2024.01.036.

16. Meredith, M. (1994). Chronic recording of vomeronasal pump activation in awake behaving hamsters. Physiol. Behav. *56*, 345–354. https://doi.org/10.1016/0031-9384(94)90205-4.

17. Døving, K.B., and Trotier, D. (1998). Structure and function of the vomeronasal organ. J. Exp. Biol. *201*, 2913–2925. https://doi.org/10.1242/jeb.201.21.2913.

18. Adams, D.R. (1992). Fine structure of the vomeronasal and septal olfactory epithelia and of glandular structures. Microsc. Res. Tech. *23*, 86–97. https://doi.org/10.1002/jemt.1070230108.

19. Salazar, I., Sánchez-Quinteiro, P., Alemañ, N., and Prieto, D. (2008). Anatomical, immnunohistochemical and physiological characteristics of the vomeronasal vessels in cows and their possible role in vomeronasal reception. J. Anat. *212*, 686–696. https://doi.org/10.1111/j.1469-7580.2008.00889.x.

20. Tirindelli, R. (2021). Coding of pheromones by vomeronasal receptors. Cell Tissue Res. *383*, 367–386. https://doi.org/10.1007/s00441-020-03376-6.

21. Iwanaga, T., and Nio-Kobayashi, J. (2020). Unique blood vasculature and innervation in the cavernous tissue of murine vomeronasal organs. Biomed. Res. *41*, 243–251. https://doi.org/10.2220/biomedres.41.243.

22. Dibattista, M., Amjad, A., Maurya, D.K., Sagheddu, C., Montani, G., Tirindelli, R., and Menini, A. (2012). Calcium-activated chloride channels in the apical region of mouse vomeronasal sensory neurons. J. Gen. Physiol. *140*, 3–15. https://doi.org/10.1085/jgp.201210780.

23. Francia, S., Pifferi, S., Menini, A., and Tirindelli, R. (2014). Vomeronasal Receptors and Signal Transduction in the Vomeronasal Organ of Mammals. In Neurobiology of Chemical Communication Frontiers in Neuroscience, C. Mucignat-Caretta, ed. (CRC Press/Taylor & Francis).

24. Hernandez-Clavijo, A., Sarno, N., Gonzalez-Velandia, K.Y., Degen, R., Fleck, D., Rock, J.R., Spehr, M., Menini, A., and Pifferi, S. (2021). TMEM16A and TMEM16B Modulate Pheromone-Evoked Action Potential Firing in Mouse Vomeronasal Sensory Neurons. eNeuro *8*. https://doi.org/10.1523/ENEURO.0179-21.2021.

25. Mohrhardt, J., Nagel, M., Fleck, D., Ben-Shaul, Y., and Spehr, M. (2018). Signal Detection and Coding in the Accessory

Olfactory System. Chem. Senses 43, 667–695. https://doi.org/10.1093/chemse/bjy061.

26. Stowers, L., Holy, T.E., Meister, M., Dulac, C., and Koentges, G. (2002). Loss of sex discrimination and male-male aggression in mice deficient for TRP2. Science 295, 1493–1500. https://doi.org/10.1126/science.1069259.

27. Tirindelli, R., Dibattista, M., Pifferi, S., and Menini, A. (2009). From pheromones to behavior. Physiol. Rev. 89, 921–956. https://doi.org/10.1152/physrev.00037.2008.

28. Zufall, F. (2005). The TRPC2 ion channel and pheromone sensing in the accessory olfactory system. Naunyn Schmiedebergs Arch. Pharmacol. 371, 245–250. https://doi.org/10.1007/s00210-005-1028-8.

29. Katreddi, R.R., Taroc, E.Z.M., Hicks, S.M., Lin, J.M., Liu, S., Xiang, M., and Forni, P.E. (2022). Notch signaling determines cell-fate specification of the two main types of vomeronasal neurons of rodents. Development 149, dev200448. https://doi.org/10.1242/dev.200448.

30. Doyle, W.I., Dinser, J.A., Cansler, H.L., Zhang, X., Dinh, D.D., Browder, N.S., Riddington, I.M., and Meeks, J.P. (2016). Faecal bile acids are natural ligands of the mouse accessory olfactory system. Nat. Commun. 7, 11936. https://doi.org/10.1038/ncomms11936.

31. Moss, R.L., Flynn, R.E., Shen, X.M., Dudley, C., Shi, J., and Novotny, M. (1997). Urine-derived compound evokes membrane responses in mouse vomeronasal receptor neurons. J. Neurophysiol. 77, 2856–2862. https://doi.org/10.1152/jn.1997.77.5.2856.

32. Sarno, N., Hernandez-Clavijo, A., Boccaccio, A., Menini, A., and Pifferi, S. (2022). Slow Inactivation of Sodium Channels Contributes to Short-Term Adaptation in Vomeronasal Sensory Neurons. eNeuro 9. https://doi.org/10.1523/ENEURO.0471-21.2022.

33. Wong, W.M., Nagel, M., Hernandez-Clavijo, A., Pifferi, S., Menini, A., Spehr, M., and Meeks, J.P. (2018). Sensory Adaptation to Chemical Cues by Vomeronasal Sensory Neurons. eNeuro 5, ENEURO.0223-18.2018. https://doi.org/10.1523/ENEURO.0223-18.2018.

34. Hafemeister, C., and Satija, R. (2019). Normalization and variance stabilization of single-cell RNA-seq data using regularized negative binomial regression. Genome Biol. 20, 296. https://doi.org/10.1186/s13059-019-1874-1.

35. Langer, S.Z., Cavero, I., and Massingham, R. (1980). Recent developments in noradrenergic neurotransmission and its relevance to the mechanism of action of certain antihypertensive agents. Hypertension 2, 372–382. https://doi.org/10.1161/01.hyp.2.4.372.

36. Tsujimoto, G., Tsujimoto, A., Suzuki, E., and Hashimoto, K. (1989). Glycogen phosphorylase activation by two different alpha 1-adrenergic receptor subtypes: methoxamine selectively stimulates a putative alpha 1-adrenergic receptor subtype (alpha 1a) that couples with Ca^{2+} influx. Mol. Pharmacol. 36, 166–176.

37. Velásquez-Martinez, M.C., Vázquez-Torres, R., and Jiménez-Rivera, C.A. (2012). Activation of alpha1-adrenoceptors enhances glutamate release onto ventral tegmental area dopamine cells. Neuroscience 216, 18–30. https://doi.org/10.1016/j.neuroscience.2012.03.056.

38. Michelotti, G.A., Price, D.T., and Schwinn, D.A. (2000). Alpha 1-adrenergic receptor regulation: basic science and clinical implications. Pharmacol. Ther. 88, 281–309. https://doi.org/10.1016/s0163-7258(00)00092-9.

39. Zhong, H., and Minneman, K.P. (1999). Alpha1-adrenoceptor subtypes. Eur. J. Pharmacol. 375, 261–276. https://doi.org/10.1016/s0014-2999(99)00222-8.

40. Insel, P.A. (1989). Structure and Function of Alpha-Adrenergic Receptors. Am. J. Med. 87, S12–S18. https://doi.org/10.1016/0002-9343(89)90108-3.

41. Holy, T.E., Dulac, C., and Meister, M. (2000). Responses of Vomeronasal Neurons to Natural Stimuli. Science 289, 1569–1572. https://doi.org/10.1126/science.289.5484.1569.

42. Kim, S., Ma, L., and Yu, C.R. (2011). Requirement of calcium-activated chloride channels in the activation of mouse vomeronasal neurons. Nat Commun. 2, 365. https://doi.org/10.1038/ncomms1368.

43. Lucas, P., Ukhanov, K., Leinders-Zufall, T., and Zufall, F. (2003). A Diacylglycerol-Gated Cation Channel in Vomeronasal Neuron Dendrites Is Impaired in TRPC2 Mutant Mice mechanism of pheromone transduction. Neuron 40, 551–561. https://doi.org/10.1016/S0896-6273(03)00675-5.

44. Zhang, P., Yang, C., and Delay, R.J. (2010). Odors activate dual pathways, a TRPC2 and a AA-dependent pathway, in mouse vomeronasal neurons. Am. J. Physiol. Cell Physiol. 298, C1253–C1264. https://doi.org/10.1152/ajpcell.00271.2009.

45. Breunig, E., Czesnik, D., Piscitelli, F., Di Marzo, V., Manzini, I., and Schild, D. (2010). Endocannabinoid modulation in the olfactory epithelium. Cell Differ. 52, 139–145. https://doi.org/10.1007/978-3-642-14426-4_11.

46. Czesnik, D., Kuduz, J., Schild, D., and Manzini, I. (2006). ATP activates both receptor and sustentacular supporting cells in the olfactory epithelium of Xenopus laevis tadpoles. Eur. J. Neurosci. 23, 119–128. https://doi.org/10.1111/j.1460-9568.2005.04533.x.

47. Eisthen, H.L., Delay, R.J., Wirsig-Wiechmann, C.R., and Dionne, V.E. (2000). Neuromodulatory effects of gonadotropin releasing hormone on olfactory receptor neurons. J. Neurosci. 20, 3947–3955. https://doi.org/10.1523/JNEUROSCI.20-11-03947.2000.

48. Mousley, A., Polese, G., Marks, N.J., and Eisthen, H.L. (2006). Terminal Nerve-Derived Neuropeptide Y Modulates Physiological Responses in the Olfactory Epithelium of Hungry Axolotls (Ambystoma mexicanum). J. Neurosci. 26, 7707–7717. https://doi.org/10.1523/JNEUROSCI.1977-06.2006.

49. McLean, J.H., Shipley, M.T., Nickell, W.T., Aston-Jones, G., and Reyher, C.K. (1989). Chemoanatomical organization of the noradrenergic input from locus coeruleus to the olfactory bulb of the adult rat. J. Comp. Neurol. 285, 339–349. https://doi.org/10.1002/cne.902850305.

50. Araneda, R.C., and Firestein, S. (2006). Adrenergic enhancement of inhibitory transmission in the accessory olfactory bulb. J. Neurosci. 26, 3292–3298. https://doi.org/10.1523/JNEUROSCI.4768-05.2006.

51. Brennan, P.A. (2004). The nose knows who's who: chemosensory individuality and mate recognition in mice. Horm. Behav. 46, 231–240. https://doi.org/10.1016/j.yhbeh.2004.01.010.

52. Brennan, P.A., Kendrick, K.M., and Keverne, E.B. (1995). Neurotransmitter release in the accessory olfactory bulb during and after the formation of an olfactory memory in mice. Neuroscience 69, 1075–1086. https://doi.org/10.1016/0306-4522(95)00309-7.

53. Doyle, W.I., and Meeks, J.P. (2017). Heterogeneous effects of norepinephrine on spontaneous and stimulus-driven activity in the male accessory olfactory bulb. J. Neurophysiol. 117, 1342–1351. https://doi.org/10.1152/jn.00871.2016.

54. Huang, G.-Z., Taniguchi, M., Zhou, Y.-B., Zhang, J.-J., Okutani, F., Murata, Y., Yamaguchi, M., and Kaba, H. (2018). α2-Adrenergic receptor activation promotes long-term potentiation at excitatory synapses in the mouse accessory olfactory bulb. Learn Mem. 25, 147–157. https://doi.org/10.1101/lm.046391.117.

55. Lorenzon, P., Antos, K., Tripathi, A., Vedin, V., Berghard, A., and Medini, P. (2023). In vivo spontaneous activity and coital-evoked inhibition of mouse accessory olfactory bulb output neurons. iScience 26, 107545. https://doi.org/10.1016/j.isci.2023.107545.

56. Smith, R.S., Weitz, C.J., and Araneda, R.C. (2009). Excitatory actions of noradrenaline and metabotropic glutamate receptor activation in granule cells of the accessory olfactory bulb. J. Neurophysiol. 102, 1103–1114. https://doi.org/10.1152/jn.91093.2008.

57. Shimazaki, R., Boccaccio, A., Mazzatenta, A., Pinato, G., Migliore, M., and Menini, A. (2006). Electrophysiological properties and modeling of murine vomeronasal sensory neurons in acute slice preparations. Chem. Senses 31, 425–435. https://doi.org/10.1093/chemse/bjj047.

58. Dibattista, M., Mazzatenta, A., Grassi, F., Tirindelli, R., and Menini, A. (2008). Hyperpolarization-activated cyclic nucleotide-gated channels in mouse vomeronasal sensory neurons. J. Neurophysiol. 100, 576–586. https://doi.org/10.1152/jn.90263.2008.

59. Amjad, A., Hernandez-Clavijo, A., Pifferi, S., Maurya, D.K., Boccaccio, A., Franzot, J., Rock, J., and Menini, A. (2015). Conditional knockout of TMEM16A/anoctamin1 abolishes the calcium-activated chloride current in mouse vomeronasal sensory neurons. J. Gen. Physiol. 145, 285–301. https://doi.org/10.1085/jgp.201411348.

60. Konno, K., Yamasaki, M., Miyazaki, T., and Watanabe, M. (2023). Glyoxal fixation: An approach to solve immunohistochemical problem in neuroscience research. Sci Adv. 9, eadf7084. https://doi.org/10.1126/sciadv.adf7084.

61. Eisinga, R., Heskes, T., Pelzer, B., and Te Grotenhuis, M. (2017). Exact p-values for pairwise comparison of Friedman rank sums, with application to comparing classifiers. BMC Bioinf. 18, 68. https://doi.org/10.1186/s12859-017-1486-2.

STAR★METHODS

KEY RESOURCES TABLE

REAGENT or RESOURCE	SOURCE	IDENTIFIER
Antibodies		
Tyrosine Hydroxylase Antibody	Miltenyi Biotec	Cat# 130-131-157; RRID:AB_2928941
Chemicals, peptides, and recombinant proteins		
Fluoromount G	Thermo Fisher Scientific	Cat# 00-4958-02
Fluo-4 AM	Invitrogen	Cat# F14217
Pluronic F-127	Invitrogen	Cat# P3000MP
Concanavalin-A	Sigma-Aldrich	Cat# C2010; CAS 11028-71-0
Prazosin hydrochloride	Sigma-Aldrich	Cat# P7791; CAS 19237-84-4
L-(−)-Noradrenaline (+)-bitartrate salt monohydrate	Sigma-Aldrich	Cat# A9512; CAS 108341-18-0
Methoxamine hydrochloride	Sigma-Aldrich	Cat# M6524; CAS 61-16-5
EGTA Ethylene glycol-bis (2-aminoethylether)-N,N,N',N'-tetraacetic acid	Sigma-Aldrich	Cat# E4378; CAS 67-42-5
BAPTA 1,2-Bis(2-Aminophenoxy)ethane-N,N,N',N'-tetraacetic acid	Sigma-Aldrich	Cat# A4926; CAS 85233-19-8
Experimental models: Organisms/strains		
Mouse: C57BL/6	Charles River	RRID:SCR_003792
Mouse BALB/c	Charles River	RRID:SCR_003792
Software and algorithms		
RStudio	Posit RStudio Desktop - Posit	RRID:SCR_000432
SEURAT	SEURAT: Visual analytics for the integrative analysis of microarray data (r-project.org)	RRID:SCR_007322
pClamp 10.6 PC software	Molecular Devices https://www.moleculardevices.com/products	RRID:SCR_011323
Clampfit 10.6	Molecular Devices https://www.moleculardevices.com/products	RRID:SCR_011323
Igor Pro software	WaveMetrics https://www.wavemetrics.com/	RRID:SCR_000325
HCImage Live	HCImage home page HCImage Live	HCImage	RRID:SCR_015041
ImageJ	National Institute of Health https://imagej.net/ij/index.html	RRID:SCR_003070
Other		
scRNA-seq data of adult VNO	Katreddi et al.[29]	NCBI GEO: GSE190330

EXPERIMENTAL MODEL AND STUDY PARTICIPANT DETAILS

Animals and ethical approval

Mice were handled according to the guidelines of the Italian Animal Welfare Act (Decreto legislativo 26/2014) and European Union guidelines on animal research (2010/63) under a protocol approved by SISSA's Animal Care Committee and the Italian Ministry of Health. Mice had free access to water and food. Every effort was made to reduce the number of animals used. C57BL/6 mice of both sexes (age range, 2–3 months)

were anesthetized by transferring to a cage (height/width/length, 8 × 10 × 12 cm), and 100% CO_2 was slowly injected into the cage until the animal stopped breathing and no longer displayed pedal reflex (near 3 min; gas flow rate, ~20% of chamber volume/min).

METHOD DETAILS

Electrophysiological recordings from VSNs in acute VNO slices

Acute slices of mouse VNO were prepared as previously described.[22,24,32,33,57] The VNO was removed and transferred to ice-cold artificial cerebrospinal fluid (ACSF). The capsule and all cartilaginous tissues were removed using fine forceps obtaining the two clean halves of the VNO. Each half was embedded in 3% agarose (A7002, Sigma-Aldrich) prepared in ACSF, once the agar had cooled to 37°C. Upon solidification, the agarose block was fixed in a glass Petri dish filled by ice-cold oxygenated ACSF solution and sliced with a vibratome (Vibratome 1000 Plus Sectioning System, Vibratome Company) at 200 μm. Slices were then left to recover for over 30 min before electrophysiological experiments were initiated.

Slices were viewed with an upright microscope (Olympus BX51WI) using infrared differential contrast optics with water immersion 20X or 60X objectives. The slice was attached to the base of the recording chamber using a home-made U-shaped silver wire and VSNs could be distinguished based on their morphology. Patch pipettes, pulled from borosilicate capillaries (WPI) with a PC-10 puller (Narishige), had a resistance ranging from 3 to 6 MΩ. Electrophysiological recordings were made using a Multiclamp 700B amplifier controlled by Clampex 10 via a Digidata 1440 (Molecular Devices). Data were low-pass filtered at 2 kHz and sampled at 10 kHz. Experiments were performed at room temperature (20–25°C). The recording chamber was continuously perfused by gravity flow with oxygenated (95% O2 and 5% CO2) ACSF.

For current-clamp recordings, the intracellular solution filling the patch pipette contained the following (in mM): 80 K-gluconate, 60 KCl, 2 Mg-ATP, 10 HEPES, and 1 EGTA, adjusted to pH 7.2 with KOH. For some experiments, 1 mM EGTA was replaced with 10 mM BAPTA. An extracellular high K^+ solution, prepared from ACSF by replacing 25 mM NaCl with KCl, was used to test the viability of neurons. Urine was collected from both sexes of C57BL/6-BALB/c mice, filtered with a 0.2 μm filter, and frozen at −80°C for no more than 2 months to maintain the integrity of pheromones. Before use, male and female urine samples were mixed in a 1:1 ratio, and the mixture was diluted to 1:50 in ACSF, pH 7.4.

A VSN was considered viable if a current injection of 3 pA elicited action potentials.

Stimuli were delivered through an 8-into-1 multibarrel perfusion pencil connected to a ValveLink8.2 pinch valve perfusion system (AutoMate Scientific). Adrenergic agonists or antagonists were applied for 3 min before starting recordings and washout was measured 5 min after removal of compounds with perfusion with ACSF, unless otherwise indicated.

Igor Pro 6.7/8 software (WaveMetrics, Lake Oswego, OR, USA) was used for data analysis.

Calcium imaging from dissociated VSNs

VSNs were dissociated using enzymatic and mechanical treatments as previously described.[22,58,59] The whole VNOs were carefully dissected and cut into 5 coronal sections under a stereoscopic microscope (Olympus SZ60) in artificial cerebrospinal fluid (ACSF) solution containing (in mM): 120 NaCl, 20 NaHCO3, 5 KCl, 2 CaCl2, 1 MgSO4, 10 HEPES, and 10 glucose, pH 7.4. VNO sections were incubated with collagenase II (1 mg/ml in PBS) for 25 minutes at 37°C, then transferred to a stop solution containing ACSF with 5% FBS. Subsequently, mechanical dissociation was performed using fire-polished glass pipettes in ACSF solution containing the Ca^{2+} indicator Fluo-4 AM (5 μM; Thermo Fisher Scientific), 0.001% pluronic F-127 (20% solution in DMSO; Thermo Fisher Scientific), and 5% FBS. Dissociated cells were plated for 1-4 hours at 4°C in dishes (FluoroDishTM; World Precision Instruments) coated with concanavalin-A (5 mg/ml) and then washed with ACSF.

Ca^{2+}-imaging experiments were performed using an epifluorescence inverted microscope with a mercury fluorescence lamp U-RF-T (IX70; Olympus). A dish containing dissociated cells was placed on the stage of the microscope and continuously perfused by gravity flow with oxygenated (95% O2 and 5% CO2) ACSF. The microscope was equipped with a Filter Block U-MWIB2 (Excitation filter EX 460-90, Dichromatic mirror DM 505, Emission filter EM 510IF) and a 40X (0.75 NA) objective (UPlanFL; Olympus). An ORCA-Flash4.0 V3 Digital CMOS camera (C13440-22CU, Hamamatsu) was used with the sotware HCImage Live (Hamamatsu). Data were acquired at 5 Hz with 512 × 512 pixel resolution. Changes in fluorescence signals were measured from specific regions of interest (ROIs) delineated around single neurons using ImageJ 1.51 s (National Institute of Health). Data were normalized and plotted as fluorescence changes: $\Delta F/F_0 = (F(t) - F_0)/F_0$, where F_0 is the average fluorescence intensity before the initial stimulus application and $F(t)$ is the fluorescence amplitude at time t. Subsequent analysis and generation of figures were conducted employing IgorPro 6.3.7.2 (Wavemetrics). A neuron was considered responsive if it satisfied the following criteria: (a) high K^+ stimulation (25 mM) induced a Ca^{2+} transient, and (b) after the stimulus, $\Delta F/F_0$ was higher than the mean intensity measured during the prestimulus (15 s), plus three standard deviations for at least 5 s. In some experiments, the reduction of fluorescence signal due to photobleaching was mathematically corrected using the exponential decay observed in non-responding cells.

Stimuli were delivered through an 8-into-1 multibarrel perfusion pencil connected to a ValveLink8.2 pinch valve perfusion system (AutoMate Scientific). Adrenergic agonists were applied for 20 s followed by 3 min washout with ACSF. Prazosin was applied for 5 min followed by 3-5 min washout with ACSF.

Single-cell RNA sequencing data analysis

Single-cell RNA sequencing (scRNA-seq) dataset was downloaded from NCBI GEO: GSE190330 and was related to the study by Katreddi et al.[29] Data consist of single cell 3' RNAseq of dissociated VNO cells from 5 male C57BL/6J mice at postnatal day 60. 10X Genomics

Chromium platform and Illumina Novaseq 6000 technology was used for sequencing. The data was analysed in R version 4.1.2 using the Seurat R package version 4.1.0, a widely used toolkit for quality control, analysis and exploration of single cell RNA sequencing data. The procedures described in Katreddi et al.,[29] with minimal modifications were used for analysing this dataset. Cells that expressed >7000 genes, <700 genes, or >10% mitochondrial genes were not included in analysis. After filtering, data from 14,851 cells were included for clustering and analysis. We used SCtransform() function as normalization method. With FindVariableFeatures() function we selected the top 2,000 highly variable genes across the population to perform principal component analysis using RunPCA(), FindNeighbors(), FindClusters() and RunUMAP() Seurat functions. The first 30 principal components were used for cell clustering, which was visualized using UMAP. We identified cell types based on known gene expression as previously shown.[29]

Immunohistochemistry

VNO tissue was dissected and immediately fixed in Glyoxal 9% + acetic acid 8% solution in PBS overnight at 4°C.[60] For cryoprotection tissue was equilibrated overnight in 30% (w/v) sucrose in PBS at 4°C. Then, the tissue was embedded in Tissue Freezing Medium (Leica Biosystems) and immediately frozen at -80°C. 20 μm coronal sections and 50 μm horizontal sections were cut on a Leica CM3050 cryostat (Leica Biosystems), mounted on Superfrost Plus slides (Menzel, Braunschweig, Germany), and stored at -20°C. To remove the cryostat embedding medium from tissue, the slices were incubated for 15 min with PBS, then incubated in blocking solution (5% normal donkey serum, 0.2% Triton X-100 in PBS) for 90 min and finally overnight at 4°C in primary antibody anti-Tyrosine Hydroxylase Vio® R667-conjugated 1:500 (Miltenyi Biotec, cat # 130-131-157). After removal of the excess of primary antibody with PBS washes, sections were incubated with DAPI (5 μg/ml) for 30 min at RT for nuclear staining. Excess of DAPI was washed and the sections were mounted in Fluoromount-G Mounting Medium (ThermoFisher, cat # 00-4958-02) Immunofluorescence was visualized with a confocal laser scanning microscope (Leica Microsystems, TCS SP5 DM6000 CFS). Images were acquired using LAS-X acquisition software (Leica Microsystems) at 1024 × 1024 pixels resolution and analyzed with ImageJ software (National Institute of Health, USA). The maximum projections of 5 μm optical slices were displayed. Control experiments, excluding primary antibodies, were performed for each immunolocalization.

Chemicals

All chemicals were obtained from Sigma-Aldrich unless otherwise specified. NA and methoxamine were prepared as 100 mM stock solutions in distilled water, while prazosin was prepared as 1 mM stock solution in methanol and diluted to the final concentrations in ACSF.

QUANTIFICATION AND STATISTICAL ANALYSIS

Igor Pro 6.3/8 software (WaveMetrics, Lake Oswego, OR, USA) was used for data analysis and figure preparation. Averaged data from individual experiments in different VSNs are presented as mean $\pm$ standard deviation (SD) along with the number of VSNs (n). The firing frequency induced by urine was calculated by the ratio between the number of spikes after urine application and the time of urine application. None of the VSNs had spontaneous spiking activity.

A VSNs was considered to have an increased firing frequency after application of NA or other compounds if satisfied the following conditions: (a) the firing frequency in the presence of the compound was >25% of that measured in control conditions (Figures 1C and 1D) and (b) after wash out the firing frequency returned below 25% of the control value. For the calculation of frequency ratios, we only used data for current injections of at least 3 pA to exclude recordings with no action potentials at lower levels of current injection.

Statistical significance was determined through the following tests. The Shapiro–Wilk test was employed to verify data normality (performed by R). For normally distributed data, repeated measures ANOVA followed by a paired t-test with Bonferroni correction (performed by Igor Pro) or mixed model two-way ANOVA followed by paired t test with Bonferroni correction (performed by GraphPad). In the case of not normally distributed data, statistical significance was assessed using Friedman's test followed by Demsar's test. The P values associated to Demsar test were calculated using the algorithm in R developed by Eisinga et al.[61] P values of <0.05 were considered statistically significant. In the Figures, * indicates P<0.05, ** P<0.001, *** P<0.0001.